SOME IMPROVED METHODS FOR REAL-TIME INTEGRATION OF STATE VARIABLE DERIVATIVES WITH DISCONTINUITIES

88-4580-CP

R. M. Howe* and A. Nwankpa**

The University of Michigan
Ann Arbor, Michigan

Abstract

In this paper we consider an analytic averaging technique for integration of discontinuous nonlinear functions. Functions with both displacement and slope discontinuities are treated. The analytic averaging method is shown to provide much better accuracy than conventional integration algorithms. This is especially true when fixed integration step sizes are used, as in real-time simulation. A simple but practical example of a bang-bang control systems is used to verify the superior performance of the analytic averaging method. It is also shown how averaging formulas for unit step and unit ramp nonlinear functions can by superposition be used to construct analytic averaging formulas for any nonlinear function which has displacement and slope discontinuities. A modified form of Euler integration is shown to be especially compatible with the analytic averaging method.

1.Introduction

In real-time simulation of dynamic systems the time derivatives of state variables sometimes have discontinuities. For example, this is clearly the case when simulating a spacecraft attitude control system which uses on-off reaction control thrusters. It is also true in the simulation of continuous controllers with effort limiting, controllers with dead-zone, etc. In general the discontinuities occur at times which are asynchronous with respect to integration step times. Because of this the use of conventional integration methods can result in substantial dynamic errors. Methods have been proposed using variable integration step size to improve the accuracy when discontinuities are present[1,2,3]. However, in real-time simulation the integration step size must be fixed and the errors introduced by discontinuous derivatives can become very serious unless the step size is made inordinately small. A technique compatible with real time simulation which utilizes an intermediate step to the discontinuity has been described and shown to exhibit high accuracy[4]. However, this method can require considerable computation time when many discontinuous functions are present in a simulation.

A less accurate but faster method for handling discontinuous nonlinear functions in fixed step integrations has also been described[5]. The method, which uses an analytic averaging technique, is introduced in the next section. A general formula for the analytic averaging function for any nonlinearity consisting of straight line segments and displacement discontinuities is developed in Section 3 from averaging formulas for unit step and unit ramp nonlinear functions. Section 4 reviews some interpolation and extrapolation methods which are useful in applying the analytic averaging method. Finally, in Section 5 we present a simple but practical example of a bang-bang control system with hysterisis to demonstrate the superior performance of the analytic averaging technique. Example solutions are shown for AB-2 integration as well as a modified form of Euler integration which turns out to be especially compatible with the analytic averaging method.

2.Derivation of the Analytic Averaging Function

Assume that a dynamic system contains a scalar state equation given by

$$\frac{dy}{dt} = f(x) \tag{1}$$

where $f(x)$ is a nonlinear function which can include discontinuities in displacement or slope. Let h be the numerical integration step. Then the ideal numerical integration formula is given by

$$y_{n+1} = y_n + \int_{nh}^{(n+1)h} f(x)\,dt = y_n + \int_{x_n}^{x_{n+1}} \frac{f(x)}{dx/dt}\,dx \tag{2}$$

Here y_n represents $y(nh)$ and x is a function of time. We next assume over the interval of integration that the time derivative of x, dx/dt, is a constant which can be approximated by the following central difference:

$$\frac{dx}{dt} = \frac{x_{n+1} - x_n}{h} = \text{constant} \tag{3}$$

Then Eq. (2) can be rewritten as

$$y_{n+1} = y_n + f_{ave}h \tag{4}$$

where

$$f_{ave} = \frac{1}{x_{n+1} - x_n}\int_{x_n}^{x_{n+1}} f(x)\,dx \tag{5}$$

With Eq. (5) we have converted the integral of $f(x)$ with respect to t in Eq. (2) to an integral of $f(x)$ with respect to x in Eq. (5). In fact f_{ave} represents simply the average value of $f(x)$ over the interval of integration. For any specified $f(x)$ the integral is a function of x_{n+1} and x_n. It can be precomputed analytically when $f(x)$ is an analytic function of x. For example, if $f(x) = x$, a linear function, the f_{ave} function is given by

$$f_{ave} = \frac{1}{x_{n+1} - x_n}\int_{x_n}^{x_{n+1}} x\,dx = \frac{x_{n+1}^2 - x_n^2}{2(x_{n+1} - x_n)} = \frac{x_{n+1} + x_n}{2} \tag{6}$$

* Professor, Department of Aerospace Engineering
Member AIAA

** Department of Aerospace Engineering

In this case we see that Eq. (4) represents trapezoidal integration. However, when $f(x)$ is a nonlinear function of x, Eqs. (4) and (5) will produce a result which is more accurate than trapezoidal integration.

It should be noted that f_{ave} as given by Eq. (5) is undefined for $x_{n+1} = x_n$. In this case it is clear that f_{ave} should be equal to f_n, the value of $f(x)$ for $x = x_n$. If it is possible for x_{n+1} to be equal to x_n in a simulation, it may be necessary to add an "if" statement in the program in order to set $f_{ave} = f_n$ when $x_{n+1} - x_n = 0$.

Figure 1 illustrates some typical discontinuous nonlinear control functions. We now proceed to derive the f_{ave} formulas for these functions.

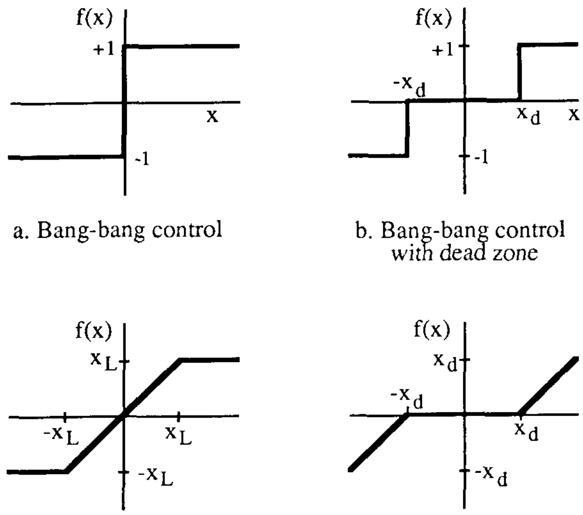

a. Bang-bang control

b. Bang-bang control with dead zone

c. Linear control with effort limiting

d. Linear control with dead zone

Figure 1. Typical controller nonlinearities.

Consider first the bang-bang switch function shown in Figure 1a. The function can be represented analytically by the formula $f(x) = x/|x|$. From Eq. (5) it follows that

$$f_{ave} = \frac{1}{x_{n+1} - x_n} \int_{x_n}^{x_{n+1}} \frac{x}{|x|} dx = |x| \Big]_{x_n}^{x_{n+1}} = \frac{|x_{n+1}| - |x_n|}{x_{n+1} - x_n} \qquad (7)$$

Note that if both x_{n+1} and x_n are positive, $f_{ave} = +1$. When both x_{n+1} and f_n are negative, $f_{ave} = -1$. When x_{n+1} and x_n have opposite polarity, f_{ave} will be somewhere between +1 and -1 and will represent the average value of the switch function over the interval x_n, x_{n+1}.

Next consider the linear function with limiting, as shown in Figure 1c. Here the function can be represented analytically by $f(x) = (|x+x_L| - |x-x_L|)/2$. From Eq. (5) we obtain the following formula for f_{ave}:

$$f_{ave} = \frac{1}{x_{n+1} - x_n} \int_{x_n}^{x_{n+1}} \frac{|x+x_L| - |x-x_L|}{2} dx$$

or

$$f_{ave} = \frac{1}{4(x_{n+1} - x_n)} \Big[(x_{n+1}+x_L)|x_{n+1}+x_L| - (x_n+x_L)|x_n+x_L| - (x_{n+1}-x_L)|x_{n+1}-x_L| + (x_n-x_L)|x_n-x_L| \Big] \qquad (8)$$

Consider next the derivation of the f_{ave} function for bang-bang control with dead zone, as illustrated in Figure 1b. Figure 2a shows how this control function can be represented as the superposition of the two bang-bang switch functions with inputs biased by $-x_d$ and x_d, respectively. It follows from Eq. (7) for the individual f_{ave} functions that the overall f_{ave} function in this case is given by

$$f_{ave} = \frac{|x_{n+1} - x_d| - |x_n - x_d| - |x_{n+1} + x_d| + |x_n + x_d|}{2(x_{n+1} - x_n)} \qquad (9)$$

Similarly, the linear function with dead zone illustrated in Figure 1d can be represented as the superposition of a linear function and an effort-limited linear function, as shown in Figure 2b. From Eq. (8) the following f_{ave} function is obtained:

$$f_{ave} = \frac{x_{n+1} + x_n}{2} - f_{LIM}(x_{n+1}, x_n) \qquad (10)$$

Here $f_{LIM}(x_{n+1}, x_n)$ is the f_{ave} function given earlier in Eq. (8) for effort-limited linear control.

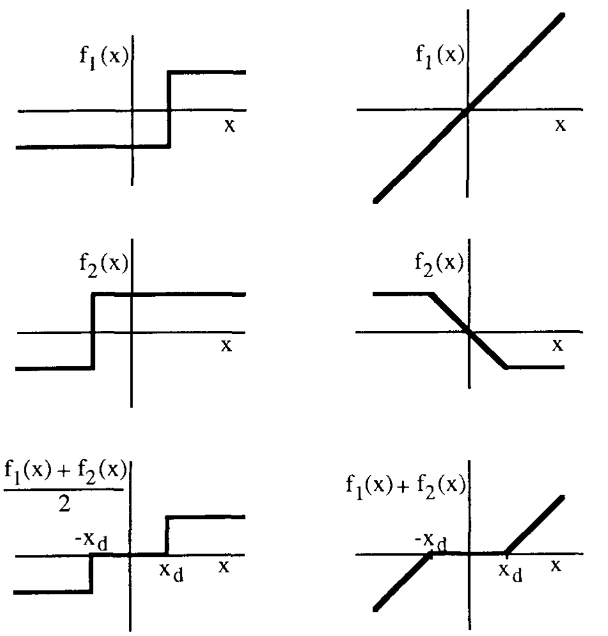

a. Synthesis of bang-bang control with dead zone

b. Synthesis of linear control with dead zone

Figure 2. Synthesis of discontinuous control functions.

3. General Synthesis of Analytic Averaging Functions

From the example in Figure 2a it is evident that symmetric nonlinear functions in general with displacement discontinuities can be synthesized by a superposition of bang-bang switch functions, each with a respective weighting constant and input bias. Also, from the example in Figure 2b it is apparent that symmetric nonlinear functions with slope discontinuities can in general be synthesized by a superposition of linear functions with limiting, each with a respective weighting constant and input limit bias. Symmetric nonlinear functions consisting of both straight-line segments and displacement jumps can be synthesized by a superposition of both linear functions with limiting and bang-bang switch functions. In all cases the corresponding f_{ave} function can be written in terms of the f_{ave} functions given by Eqs. (7) and (8).

We next consider asymmetric nonlinear functions with displacement discontinuities. These can in general be synthesized by a superposition of step functions. The individual unit step function $d(x)$ in Figure 3a can be represented analytically by the formula $d(x) = (1+x/|x|)/2$. From Eq. (5) the corresponding f_{ave} function, which we denote as $D(x_{n+1}, x_n)$, is given by

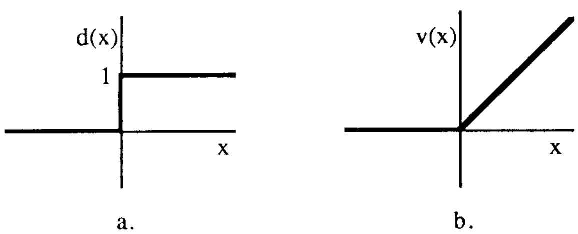

Figure 3. Unit step and ramp functions.

$$d_{ave} = D(x_{n+1}, x_n) = \frac{1}{2} + \frac{|x_{n+1}| - |x_n|}{2(x_{n+1} - x_n)} \tag{11}$$

Any staircase-type discontinuous function can be represented as the sum of biased step functions. Thus we can write

$$f(x) = f_0 + \sum_{i=1}^{N} k_i d(x - x_i) \tag{12}$$

It follows from Eq. (11) that the corresponding f_{ave} function can be computed from the formula

$$f_{ave} = f_0 + \sum_{i=1}^{N} k_i D_i(x_{n+1} - x_i, x_n - x_i) \tag{13}$$

Any asymmetric nonlinear function consisting of straight-line segments can be synthesized by a superposition of ramp functions. The individual unit ramp function $v(x)$ in Figure 3b can be represented by the formula $v(x) = (x+|x|)/2$. From Eq. (5) the corresponding f_{ave} function $V(x_{n+1}, x_n)$ is given by

$$f_{ave} = V(x_{n+1}, x_n) = \frac{x_{n+1}(x_{n+1} + |x_{n+1}|) - x_n(x_n + |x_n|)}{4(x_{n+1} - x_n)} \tag{14}$$

The general segmented function can be written as

$$f(x) = f_0 + m_0 x + \sum_{i=1}^{M} m_i v(x - x_i) \tag{15}$$

Thus the corresponding f_{ave} function is computed from the formula

$$f_{ave} = f_0 + m_0 \frac{x_{n+1} - x_n}{2} + \sum_{i=1}^{M} m_i V(x_{n+1} - x_i, x_n - x_i) \tag{16}$$

Eqs. (11) through (16) can be built into a computer subroutine which will automatically calculate the $f_{ave}(x_{n+1}, x_n)$ function given the data points defining any nonlinear function $f(x)$ that consists of linear segments plus displacement discontinuities.

4. Methods for determining x_{n+1}

It is clear from Eq. (5) that f_{ave} will be a function of x_{n+1} and x_n. When f_{ave} is computed during the nth integration frame, x_{n+1} may not be available. In this case it will be necessary to estimate x_{n+1}. In this section we consider several methods for making this estimate and the associated accuracy of the estimate. In the following sections specific examples will be used to illustrate several of the methods.

If x_n is a state variable or a known function of state variables, it may be possible to perform the state variable integrations during the nth frame prior to computing the f_{ave} function. In this case x_{n+1} will represent the most accurate estimate possible that is consistant with the algorithm being used for numerical integration. If it is not possible to obtain x_{n+1} in this fashion, then it must be estimated using some type of extrapolation algorithm.

Again, if x_n is a state variable, the time derivative $\dot{x}_n$ will be available for the estimate of x_{n+1}. If, alternatively, x_n is an analytic function of state variables, then $\dot{x}_n$ can be calculated, although for complex functions the calculation may not be trivial. In any event let us assume that $\dot{x}_n$ is available or can be computed. Then a first-order power series extrapolation formula for x_{n+1} is the following:

$$x_{n+1} = x_n + h\dot{x}_n \tag{17}$$

From the Taylor series representation for x_{n+1} in terms of x_n it is easily seen that the error in x_{n+1} is approximately $-\ddot{x}_n h^2/2$. It is apparent that the extrapolation formula of Eq. (17) is identical with the Euler integration formula.

A second method for estimating x_{n+1} uses linear extrapolation based on x_n and x_{n-1}. Here the formula is

$$x_{n+1} = 2x_n - x_{n-1} \tag{18}$$

In this case the error in x_{n+1} is approximately $-\ddot{x}_n h^2$, i.e., twice the error associated with the estimate of Eq. (17).

A second-order extrapolation method for x_{n+1} is based on x_n, x_{n+1} and $\dot{x}_n$. Here the formula is given by

$$x_{n+1} = x_{n-1} + 2h\dot{x}_n \tag{19}$$

Here the error in x_{n+1} is approximately $-\dddot{x}_n h^3/3$.

Other higher order extrapolation algorithms can of course be considered[6]. Because of the asumption that dx/dt is constant in the derivation of the f_{ave} foumula, however, it is doubtful if much would be gained in going to more accurate extrapolation methods.

5. Bang-bang Control system Example

In this section we consider an example simulation of a dynamic system with discontinuities. Figure 4 shows a block diagram of the system, which consists of a pure inertia plant driven by a "bang-bang" controller with hysterisis. Proportional plus rate control is mechanized with the lead-lag filter shown in the figure. If the controller were also to include deadzone, the system would be representative of a typical spacecraft single-axis attitude control system.

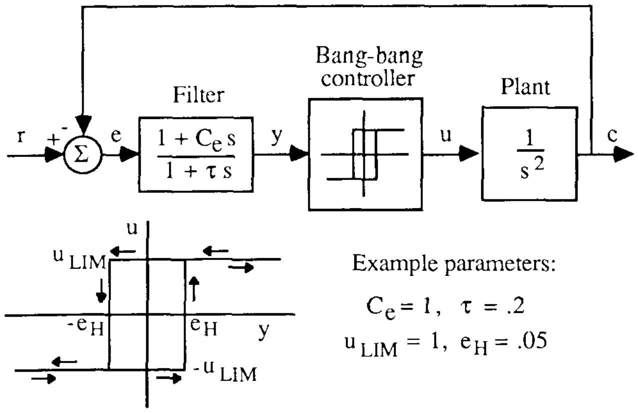

Figure 4. Bang-bang control system with hysterisis.

For the parameters shown in the figure the time response of the control system for zero input ($r = 0$) and two different initial conditions, $c(0)$, is shown in Figure 5. The other two states are initially zero. Note that the response approaches a limit cycle in each case. This is of course typical for any bang-bang control system.

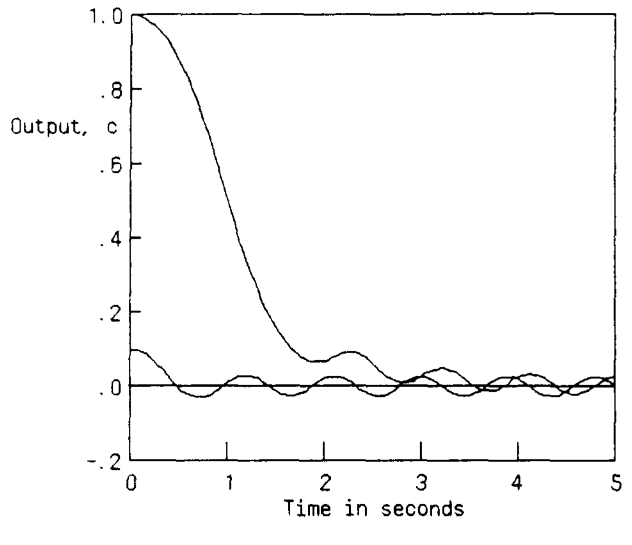

Figure 5. Transient response of control system for two different initial conditions.

The control system is described by the following state equations:

$$\dot{x} = \frac{1}{\tau}(r - c - x), \quad y = x + C_e\dot{x}, \qquad u = u_{LIM}\frac{y \pm e_H}{|y \pm e_H|}, \quad \dot{c}_d = u, \quad \dot{c} = c \tag{20}$$

We consider first the simulation of the system using the second-order Adams-Bashforth (AB-2) predictor algorithm, which is probably the most popular real-time integration method. This results in the following difference equations when the standard method for nonlinear function evaluation is employed:

$$x_{n+1} = x_n + \frac{h}{2}(3fx_n - fx_{n-1}), \quad fx_n = r_n - c_n - x_n$$

$$y_n = x_n + C_e fx_n, \quad S_n = \frac{y_n + e_H S_{n-1}}{|y_n + e_H S_{n-1}|}, \quad u_n = u_{LIM}S_n \tag{21}$$

$$c_{d_{n+1}} = c_{d_n} + \frac{h}{2}(3u_n - u_{n-1}), \quad c_{n+1} = c_n + \frac{h}{2}(3c_{d_n} - c_{d_{n-1}})$$

Here we have introduced a discrete state variable $S_n = \pm 1$ in order to mechanize the hysterisis bias e_H, where the polarity of the bias depends on the previous switch state, S_{n-1}.

Next we replace the conventional evaluation of the bang-bang control function u_n with the f_{ave} function in accordance with Eq. (7). The formula for the switch variable S_n given in Eq. (21) is still retained to preserve the evaluation of the hysterisis bias $\pm e_H$. But the equations for u_n and $c_{d_{n+1}}$ are replaced by

$$\tilde{u}_{n+1/2} = u_{LIM}\frac{|y_{n+1} + e_H S_{n-1}| - |y_n + e_H S_{n-1}|}{y_{n+1} - y_n}, \tag{22}$$

$$c_{d_{n+1}} = c_{d_n} + h\tilde{u}_{n+1/2} \tag{23}$$

In Eq. (22) we have denoted the f_{ave} function by $\tilde{u}_{n+1/2}$. This is because the average value of the bang-bang control over the interval from nh to (n+1)h is equivalent to an estimate of u halfway through the interval as it is used in the integration algorithm of Eq. (23).

In Figure 6 the error in the simulated control system output c when using AB-2 integration for $c(0) = 1$ is plotted as a function of time. Two cases are shown. In one case AB-2 is used with the standard method of bang-bang function evaluation, as represented by the difference equations in (21). In the second case the function averaging method is used to represent and integrate the bang-bang control, as reflected by Eqs. (22) and (23). Use of the averaging method has clearly made a very significant improvement in the accuracy of the solution. It should be noted that in both cases the AB-2 algorithms were started so that there was no error for the initial 1 second portion of the solution, over which the controller output u is equal to -1. It is when u switches from -1 to +1 and when subsuquent switches in u occur that the error transients are generated.

Eq. (23) can be viewed as a modified form of Euler integration wherein the half integer state variable derivative at $n+1/2$ instead of the derivative at the integer n is utilized in computing the $n+1$ state. This form of modified Euler integration can actually be used for many if not all integrations in

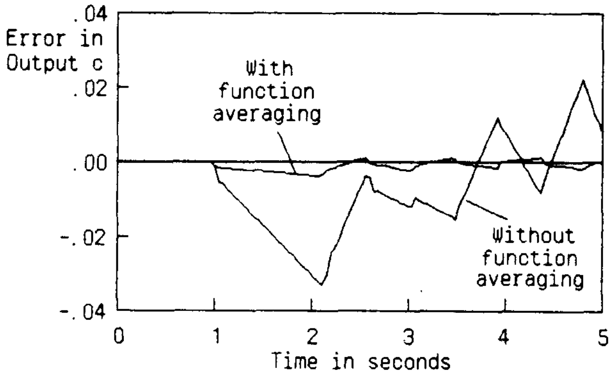

Figure 6. Error in control system output when using AB-2 integration.

a simulation. It has the advantage that the dynamic errors associated with the method are proportional to $h^2/24$, compared with $5h^2/12$ for AB-2 integration(7). For this reason and because of its compatibility with the function averaging method for handling discontinuities, we next consider the modified Euler method for all integrations in the simulation of our bang-bang control system.

When applying modified Euler integration it is necessary to designate some of the state variables at half integer rather than integer time steps. For the control system example here we choose to represent the output position c at integer steps, with the output velocity c_d and the filter state x represented at half-integer steps. When the standard method for nonlinear function evaluation is used, the modified Euler difference equations for simulating the control system state equations in (20) become the following:

$$x_{n+1/2} = A_x x_{n+1/2} + B_x(r_n - c_n)\,, \quad A_x = \frac{1-\frac{h}{2\tau}}{1+\frac{h}{2\tau}}\,, \quad B_x = \frac{\frac{h}{\tau}}{1+\frac{h}{2\tau}} \tag{24}$$

$$y_n = \tilde{x}_n + \frac{C_e}{\tau}(r_n - c_n - \tilde{x}_n)\,, \quad \tilde{x}_n = \frac{x_{n+1/2} + x_{n-1/2}}{2} \tag{25}$$

$$S_n = \frac{y_n + e_H S_{n-1}}{|y_n + e_H S_{n-1}|}\,, \quad u_n = u_{LIM} S_n \tag{26}$$

$$c_{d_{n+1/2}} = c_{d_{n-1/2}} + h u_n\,, \quad c_{n+1} = c_n + h c_{d_{n+1/2}} \tag{27}$$

We note in Eq. (24) that modified Euler has been used to integrate $(r_n - c_n - \tilde{x}_n)/\tau$ and thus obtain $x_{n+1/2}$ from $x_{n-1/2}$. Here the estimate $\tilde{x}_n$ is obtained by averaging $x_{n+1/2}$ and $x_{n-1/2}$, as shown in Eq. (25). In this case we are in effect using trapezoidal integration for the state x. The resulting difference equation is solved explicitly for $x_{n+1/2}$, which leads to Eq. (24) with the coefficients A_x and B_x. The estimate $\tilde{x}_n$ is also used in Eq. (25) for the filter output y_n, which in turn is used in Eq. (26) to compute the bang-bang switch output S_n and hence the controller output u_n. In Eq. (27) the velocity $c_{d_{n+1/2}}$ is computed from $c_{d_{n-1/2}}$ using u_n with modified Euler integration, as is c_{n+1} from c_n using $c_{d_{n+1/2}}$.

To employ the function averaging method with modified Euler integration we utilize the following equations for the calculation of $\tilde{u}_n$, the average value of u over the interval from $(n-1/2)h$ to $(n+1/2)h$:

$$\tilde{u}_n = u_{LIM} \frac{|\tilde{y}_{n+1/2} + e_H S_{n-1}| - |\tilde{y}_{n-1/2} + e_H S_{n-1}|}{\tilde{y}_{n+1/2} - \tilde{y}_{n-1/2}} \tag{28}$$

where

$$\tilde{y}_{n+1/2} = \frac{3}{2}y_n - \frac{1}{2}y_{n-1}\,, \quad \tilde{y}_{n-1/2} = \frac{y_n + y_{n-1}}{2} \tag{29}$$

In Eq. (28) for $\tilde{u}_n$ the formula is based on estimates $\tilde{y}_{n+1/2}$ and $\tilde{y}_{n-1/2}$, as obtained in Eq.(29) from y_n and y_{n-1} using first-order extrapolation and interpolation, respectively. To use modified Euler integration with function averaging for the bang-bang control, then, $\tilde{u}_n$ is employed instead of u_n in Eq. (27).

In Figure 7 the error in simulated control system output c when using modified Euler integration for $c(0) = 1$ is plotted versus time. As before, two cases are shown, one without the averaging method and the second using the averaging method, as mechanized with Eqs. (28) and (29). Again we note the very substantial accuracy improvement when using the function averaging algorithm.

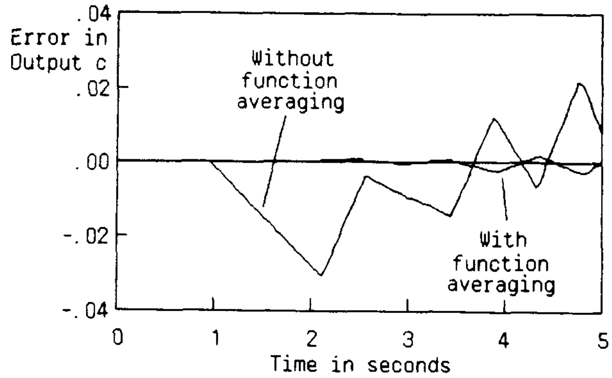

Figure 7. Error in control system output when using modified Euler integration.

Although the accuracies observed in Figure 6 for AB-2 integration are comparable with those in Figure 7 for modified Euler integration, the modified Euler has some advantags over the AB-2 implementation. In particular, the AB-2 mechanization in Eq. (22) requires y_{n+1} and therefore r_{n+1} for the nth integration frame. If r is a real-time input, r_{n+1} will not be available, although it could be estimated from r_n and r_{n-1} by extrapolating ahead by h seconds. On the other hand, in the modified Euler mechanization in Eqs. (28) and (29) y_{n+1} and hence r_{n+1} is not required. Thus the simulation will be compatible with real-time inputs. It is true in this case that extrapolation in Eq. (29) is required in computing $\tilde{y}_{n+1/2}$, but it is extrapolation over the interval $h/2$ rather than h. This reduces the extrapolation error by a factor of four. We might also note that when the lead-lag filter has a second-order lag, i.e., a transfer operator given by $(1+C_e s)/(1+\tau s)^2$, the modified Euler algorithm permits the calculation of $y_{n+1/2}$ without the use of extrapolation.

We have also noted earlier in this section that the modified Euler method in general has a dynamic accuracy which is an order of magnitude better than AB-2 (error coefficient proportional to $h^2/24$ compared with $5h^2/12$). In the bang-bang control system example used here the dynamic errors are dominated by the errors associated with the discontinuous control function. Indeed, this is why the function averaging method made such a dramatic improvement in the accuracy. Because of this, however, the poorer overall accuracy of AB-2 is not so evident, especially when we note that AB-2 produces an exact result when simulating our pure inertia plant with a constant input. In more complex problems the authors have found that the modified Euler method enjoys a substantial accuracy advantage over AB-2[7].

Finally, there are fewer startup problems associated with modified Euler integration. In particular, the initial integration step for the half integer states $x_{n+1/2}$ and $c_{d_{n+1/2}}$ starting with x_0 and c_{d_0} is taken as $h/2$ rather than h. Normally AB-2 is started with Euler integration for the first step, which introduces a substantial error transient. To obtain the accuracy shown in Figure 6 we were forced to compute startup deriva-tives at $t = -h$. In general this may be inconvenient.

Previous studies of the function averaging technique described in this paper have also shown impressive accuracy improvement when the method is used in handling slope discontinuities, e.g., for effort-limited linear controllers, as well as the displacement discontinuities of bang-bang controllers[3]. These studies have demonstrated that the function averaging technique can be used successfully in conjunction with other integration methods such as AB-3, AB-4, RK-2 and RK-4. The previous studies have also shown that the errors resulting from both types of discontinuities are strongly dependent on the time at which the discontinuity occurs during the interval between nh and $(n+1)h$. It follows that small changes in the initial conditions in the example considered here will make substantial changes in the size of the error transients, especially for the cases where the function averaging method is not used. Hence the results in Figures 6 and 7 should only be considered as typical, not all encompassing.

6. Conclusions

The use of an analytic averaging technique improves considerably the accuracy in simulating dynamic systems with discontinuous state-variable derivatives. The method is especially effective for fixed integration step sizes, such as are used in real-time simulation. The improved accuracy has been demonstrated in the simulation of a bang-bang control system with hysterisis for both AB-2 integration and a modified form of Euler integration. The analytic averaging formulas for applying the method to any nonlinear function consisting of linear segments and displacement discontinuities have been presented.

7. References

1. Carver, M.B., "Efficient Integration over Discontinuities in Ordinary Differential Equations," *Mathematics and Computers in Simulation*, vol. xx, no. 3, pp 190-196, 1978.
2. Ellison, D., "Efficient Automatic Integration of Ordinary Differential Equations with Discontinuities," *Mathematics and Computers in Simulation*, vol. xxiii, no. 1, pp 12-20, 1981.
3. Halin, H.J., "Integration Across Discontinuities in Ordinary Differential Equations Using Power Series," *Simulation*, vol. 32, no. 2, pp 33-45, 1979.
4. Howe, R.M., X.A. Ye and B.H. Li, "An Improved Method for Simulation of Dynamic Systems with Discontinuous Nonlinearities," *Trans. of the Society for Computer Simulation*, Vol.2, No. 1, pp 169-187, 1985.
5. Howe, R.M., "A New Method for Handling Discontinuous Nonlinear Functions in Digital Simulation of Dynamic Systems," *Proc 1978 Summer Computer Simulation Conference*, pp 72-79, The Society for Computer Simulation, P.O. Box 17900, San Diego, CA 92117.
6. Howe, R.M., "Dynamics of Digital Extrapolation and Interpolation," *Trans. of the Society for Computer Simulation*, Vol.2, No. 1, pp 169-187, 1985.
7. Howe, R.M., "The Role of Modified Euler Integration in Real-time Simulation," *Proceedings of the Conference on Aerospace Simulation III*, San Diego, 1988; pp 277-285. The Society for Computer Simulation, P.O. Box 17900, San Diego, CA 92117.